

# We are IntechOpen, the world's leading publisher of Open Access books Built by scientists, for scientists

6,900

Open access books available

185,000

International authors and editors

200M

Downloads

Our authors are among the

154

Countries delivered to

TOP 1%

most cited scientists

12.2%

Contributors from top 500 universities



WEB OF SCIENCE™

Selection of our books indexed in the Book Citation Index  
in Web of Science™ Core Collection (BKCI)

Interested in publishing with us?  
Contact [book.department@intechopen.com](mailto:book.department@intechopen.com)

Numbers displayed above are based on latest data collected.  
For more information visit [www.intechopen.com](http://www.intechopen.com)



# Optimized Model Updating of a Railway Bridge for Increased Accuracy in Moving Load Simulations

Johan Wiberg, Raid Karoumi and Costin Pacoste  
*KTH Royal Institute of Technology  
 Sweden*

## 1. Introduction

The moving load problem has been studied intensively since the first research by Willis in 1849 (Willis, 1850). Today's railway bridges are analyzed in more detail for moving loads due to increased speeds, axle loads and more slender bridge designs. Such analyses are very time consuming as it involves many simulations using different train configurations passing at different speeds. Thus, simplified bridge and train models are chosen for time efficient simulations. However, these FE models are often called into question when they are in conflict with in-situ bridge measurements. Model updating has therefore been a rapidly developing technology and has gained a lot of interest in recent years. It is the popular name for using measured structural data to correct the errors in FE models. Clearly, the approach of numerical predictions to the behavior of a physical system is limited by the assumptions used in the development of the mathematical model (Friswell & Mottershead, 1995). Model updating, at its most ambitious, is about correcting invalid assumptions by processing test results.

Mottershead & Friswell (1993) provided a state of the art and addressed the problem of updating a numerical model by using data acquired from a physical vibration test (Friswell & Mottershead, 1995). Optimization has been used by many others since then, improving FE model predictions based on real measurements. This chapter highlights the importance and the potential of such optimization procedures for increased accuracy in moving load simulations. A large-scale simplified railway bridge FE model is used and the updating process is based on previously identified updating parameters in Wiberg et al. (2009). Natural frequency, static strain, static deflection and acceleration residuals are used, separately and combined, to optimize the values of modulus of elasticity, mass density and modal damping ratio. The updated FE model is finally used to identify and analyze the most critical moving load configuration in CEN (2002) concerning bending moment, vertical bridge deck deflection and acceleration.

The optimization algorithm was easily implemented for FE model updating and was shown to operate efficiently in a benchmark test and for the specific bridge. The optimization algorithm converges against reasonable values of the updating parameters. A previously questioned high-valued equivalent modulus of elasticity, found for a manually tuned FE model in Wiberg (2009), was proven to be reliable. Further, the difference in load effect between an initial manually tuned FE model and the optimized FE model is found most significant for vertical deflection. However, more measured dynamic characteristics (natural frequencies, mode

shapes and modal damping ratios), together with complementing updating parameters and a more detailed FE model are considered necessary for dynamic load effect predictions with highest accuracy.

Finally, it should be given attention that the adopted methodology can not only be used for model updating based on measurements, but also introduced in the early design phase. The reasonable range of a typical modeling factor or parameter is then based on the drilled engineer's qualified guess and the risk of for example a resonance problem can be investigated by, e.g. letting the maximum allowed code limit for vertical bridge deck acceleration be "measured" response. Performing the optimization will then result in a model configuration, needed to fulfill the requirements in the code.

## 2. FE model optimization

### 2.1 General

The objective of FE model updating is to improve an FE model in order to reproduce the measured response of a structure. Model updating brings together the skills of the numerical analyst and the load test engineer, and requires the application of modern estimation techniques to produce the desired improvement (Friswell & Mottershead, 1995). Basically, an understanding of the updated model is necessary. The updated model may only reproduce physical test data but could lack physical meaning. It is therefore required to accurately know the application area of the updated model. Typically, the physical meaning of the model must be improved if the updated model is to assess the effect of changes in construction.

Optimization techniques are used to find a set of design parameters,  $\mathbf{p} = \{p_1, p_2, \dots, p_n\}$ , that can somehow be defined as optimal. FE modeling procedures involve an optimization with respect to an objective function, i.e. finding an optimal model that behaves similarly to the real structure and represents the physical characteristics of it (Zárate & Caicedo, 2008). Thus, residuals of the response, as a nonlinear function of the input parameters, are established and accounted for in the objective function. Different types of objective functions are found in the literature and by their minimization an FE model may be optimally updated.

The optimization process is rather straightforward. More complex is the choice of updating parameters, i.e. those exerting an influence on the bridge model in question. It is reasonable to believe that an accurate representation of a structure depends on the type of FE model used to represent the structural members and the properties assigned to these elements. Therefore, relatively large differences can exist between the behavior of a FE model before updating and the real structure.

Considering the minimization problem as unconstrained nonlinear, i.e. finding a vector  $\mathbf{p}$  that is local minimum to a scalar function  $\Pi(\mathbf{p})$ :

$$\min_{\mathbf{p}} \Pi(\mathbf{p}) \quad (1)$$

with no restriction placed on the range of  $\mathbf{p}$ , the Nelder-Mead simplex algorithm as described in Lagarias et al. (1998) can be used for optimization. The algorithm is capable of escaping local minima in some cases and can even handle discontinuities (Coleman & Zhang, 2009). Unlike gradient based optimization routines, facing ill-conditioning for the Jacobian and

Hessian matrices, the Nelder-Mead simplex algorithm is less prone to numerical difficulties at iteration steps. Also for noisy measurements the Nelder-Mead simplex algorithm has been proven effective, see e.g. the updating results of a simple beam in Jonsson & Johnson (2007) or the more extensive study of Schlune et al. (2009) to improve the FE model of the new Svinesund Bridge between Sweden and Norway. Further, the optimization algorithm is general, problem independent and can be implemented easily for FE model updating.

## 2.2 The objective function

The objective function is the crucial heart of FE model updating. It represents the magnitude of the error of the response vector,  $\mathbf{z}$ , defined as the difference between the observed responses and the expected responses  $E\{\mathbf{z}\}$  (Friswell & Mottershead, 1995):

$$\Pi = E\left\{(\mathbf{z} - E\{\mathbf{z}\})^T (\mathbf{z} - E\{\mathbf{z}\})\right\} \quad (2)$$

Typically, the response residual vector is weighted to reflect the confidence in different measurements:

$${}^z\Pi = (\mathbf{z}_m - \mathbf{z}_j)^T \mathbf{W}_z (\mathbf{z}_m - \mathbf{z}_j) \quad (3)$$

where  $\mathbf{z}_m$  is the measured response vector,  $\mathbf{z}_j$  is the FE response vector at iteration  $j$  and the response weighting matrix,  $\mathbf{W}_z$ , is a diagonal matrix with corresponding reciprocals as diagonal elements depending on the type of objective function. Notations are also to be found in Appendix 5.1.

The selection of the objective function has a profound impact on the problem (Jaishi & Ren, 2005). A classical least squares approach fails to acknowledge that the observations are not recorded with equal confidence (Friswell & Mottershead, 1995). In reality, different error sources will also reduce the ability of the FE model to reproduce the experimental measurements. This can be systematic errors, experimental noise and modeling limitations. In a weighted least squares approach each squared measurement residual is therefore multiplied by a weight,  $w_i$ , and the sum of weighted squares of the residuals is calculated. When the weights are given by the inverse observation variances,

$$\mathbf{W} = \text{diag}\left(\frac{1}{\sigma_1^2}, \frac{1}{\sigma_2^2}, \dots, \frac{1}{\sigma_i^2}, \dots, \frac{1}{\sigma_{N_z}^2}\right) \quad (4)$$

the minimization problem,  $\min_{\mathbf{p}} {}^z\Pi$ , has the objective function:

$${}^z\Pi = \sum_{i=1}^{N_z} \sqrt{\frac{(z_{mi} - z_i)^2}{\sigma_{z_i}^2}} = \sum_{i=1}^{N_z} \frac{|z_{mi} - z_i|}{\sigma_{z_i}} \quad (5)$$

This is the objective function used by Jonsson & Johnson (2007) and Schlune et al. (2009). To keep the least squares form of the objective function, the square root is omitted and the objective function reformulated as:

$${}^z\Pi = \sum_{i=1}^{N_z} \frac{(z_{mi} - z_i)^2}{\sigma_{z_i}^2} = (\mathbf{z}_m - \mathbf{z}(\mathbf{p}_j))^T \mathbf{W}_z (\mathbf{z}_m - \mathbf{z}(\mathbf{p}_j)) \quad (6)$$

which corresponds to Eq. 3 with possibility to take the significance of different measurements into account and with dimensionless terms as a result. The normalized updating parameter vector is defined as

$$\mathbf{p}_j = \left( \frac{p_{1,j}}{p_{1,0}}, \frac{p_{2,j}}{p_{2,0}}, \dots, \frac{p_{n,j}}{p_{n,0}} \right) \quad (7)$$

### 2.3 Optimization procedure

FE model updating becomes very efficient, neat and easy to implement by coupling the FE analysis software in question to a mathematical analysis software such as the Matlab® package. This also most conveniently facilitate the use of the Matlab® incorporated optimization toolbox and the updating process is therefore fully controlled from within Matlab®. In order to use a typical optimization solver, a function handle of the objective function together with an initial normalized updating parameter vector are sent to the optimization subroutine. The updated FE model code is then automatically generated by the optimization algorithm as it iterates. The Matlab® syntax for a general and problem independent optimization procedure is then:

```
% Response function as function handle @:
z=@(p) FEA(p) ;

% Objective function as function handle @:
obj=@(p) obj_func(zm,z,sigma) ;

% Initial normalized updating parameter vector:
p0=[1 1] ;

% Nelder-Mead simplex optimization based on functions Z and OBJ:
[p,objval,exitflag,output]=fminsearch(obj,p0,options) ;
```

In this case FEA(p) includes the appropriate code for initiation of the finite element analysis and calculation of the response vector as a function of the updating parameter vector p from the optimization solver fminsearch in the optimization toolbox of Matlab®. In this case the Solvia® FE system software was adopted.

The optimization algorithm starts at the point p0 and attempts to find a local minimum p of the function described in obj, with measured response zm, standard deviations in responses sigma and optimization options specified in options. The algorithm returns in objval the value of the objective function obj at the solution p, in exitflag the exit condition of fminsearch and in output the user specified information about the optimization are found.

### 3. Benchmark test

A benchmark test was performed to verify the updating procedure implemented in Matlab®. The physical problem consisted of a 2D dynamic analysis of a moving vehicle across a ballasted railway bridge with vehicle-bridge interaction due to contact definitions, see Fig. 1. The I-beam steel bridge had two spans, assumed to be linearly elastic, and the vehicle speed was 30 m/s. The bridge surface and the neighboring rigid surface portions are assumed to initially form a horizontal straight line. Each span was modeled to consist of 20 beam elements and a mass-spring-damper system was used to model the vehicle. The mass density

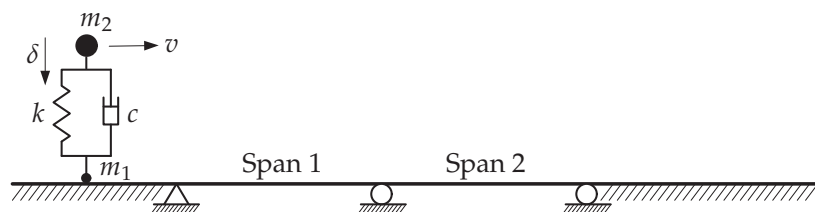


Fig. 1. The physical benchmark problem.

of the beam was increased to include the mass of the ballast. Direct time integration with the Hilber method was adopted. All necessary input data to the Solvia® FE system is given in Appendix 7.

To symbolize “measured” result, material properties of 210 GPa and 16000 kg/m<sup>3</sup> for modulus of elasticity and mass density, respectively, were used and the corresponding “measured” maximum deflection in each span was calculated to 2.152 mm and 2.165 mm. In addition to these “measured” responses, the predicted finite element analysis responses, as a function of the iteratively updated material properties, constituted the objective function expression. For simplicity, the Euclidean norm of the normalized response residual was chosen as objective function:

$$z_{\Pi} = \sqrt{\sum_{i=1}^{N_z} \frac{(z_{mi} - z_i)^2}{z_{mi}^2}} = \left\| \frac{\mathbf{z}_m - \mathbf{z}(\mathbf{p}_j)}{\mathbf{z}_m} \right\| \quad (8)$$

Using the modulus of elasticity and mass density as updating parameters, with initial values of 175 GPa and 20000 kg/m<sup>3</sup>, i.e. corresponding to initial deflections of 2.658 mm and 2.607 mm, the `fminsearch` solver in Matlab® converged towards 210 GPa and 16000 kg/m<sup>3</sup> at the deflections 2.152 mm and 2.165 mm in 30 iterations and 62 objective function counts. Fig. 2 illustrates the iteration sequence, starting at the normalized input parameter coordinates  $(\frac{175}{175}, \frac{20000}{20000})$  and ending at  $(\frac{210}{175}, \frac{16000}{20000})$ . Interestingly, the algorithm first seemed to localize a local minimum but proceeded to the global minimum.

#### 4. Case study

The New Årsta Bridge in Stockholm, Sweden, was adopted for FE model updating (see Fig. 3). Previous research pointed out some of the difficulties in studying bridge dynamics resulting from moving traffic (Wiberg et al., 2009). Not only does the dynamic amplification depends on the considered load effect, but different modeling parameters, individually or jointly, influence the dynamic load effect or dynamic property in question. The use of statistically identified updating parameters as a step in more effective model optimization is highlighted in previous study by the author and typical results from a statistical parameter study on this specific bridge are exemplified in Fig. 4 and found in Wiberg et al. (2009) where the factorial experimentation technique was used. The type of information encountered in Fig. 4 is considered extremely important and valuable. Thus, the statistical method of factorial experimentation, in contrast to ordinary parameter sensitivity analyzes where parameters are varied one at a time, captures the synergy effects. Consequently, a modeling parameter can be significant even though it individually is found insignificant and an optimal amount of updating parameters to include in the optimization can therefore be identified. This leads to shorter solution times as the optimization algorithm itself is iterative and becomes



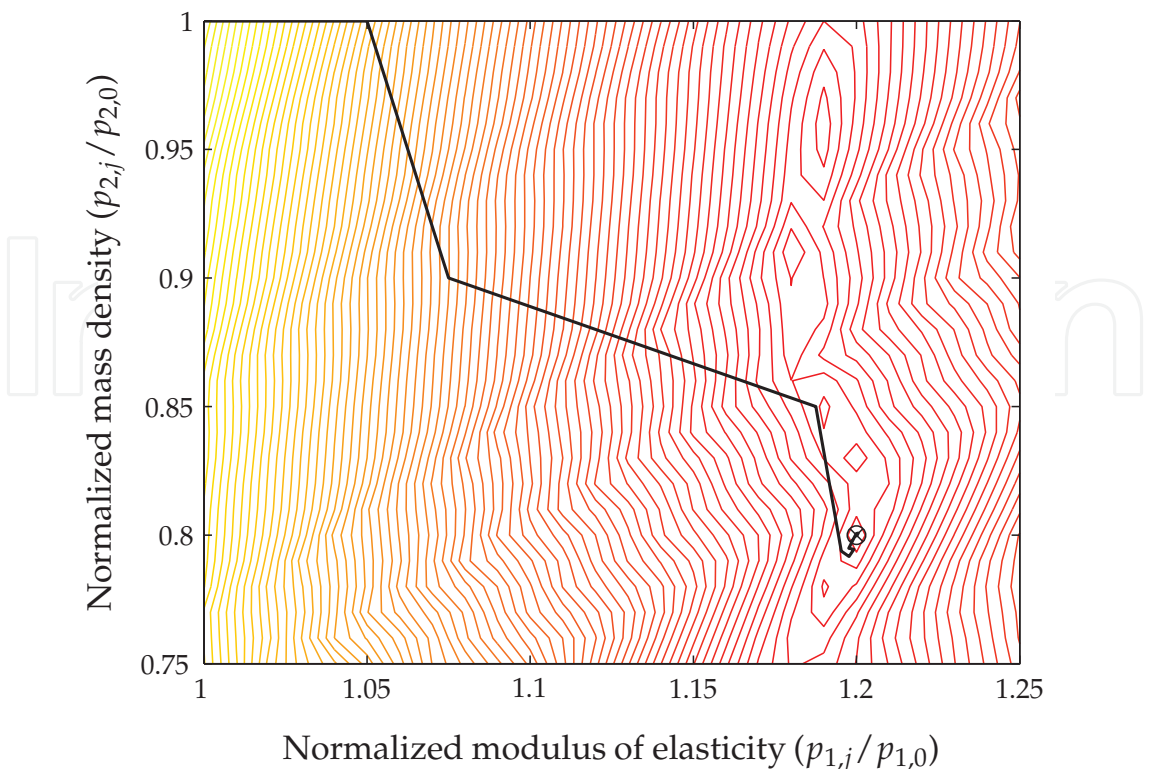


Fig. 2. Sequence of updating parameter points in the normalized updating parameter space. The contours represent the magnitude of the response objective function.

very time-consuming for large dynamic simulations with inappropriately many updating parameters causing unnecessarily many iterations.

A large-scale simplified bridge FE model in the Solvia® FE system was verified as reliable for global analysis and manually tuned concerning an equivalent modulus of elasticity and mass density by using operational modal analysis and static load tests (Wiberg, 2006; 2007; 2009; Wiberg & Karoumi, 2009). This 3D modified Bernoulli-Euler beam model was therefore used as a basis for the present study.

4.1 The bridge

The eleven span New Årsta Bridge of approximately 815 m has main spans of 78 m. Elevation and plan view with the monitoring sections is presented in Fig. 5. The cross section of the bridge is complex with a parabolic height variation. To make the slender design possible, the sections were extensively reinforced and prestressed. To use a simplified inclusion of tendons in the model, they were concentrated to the center of gravity along the bridge and not distributed within the cross section. Further, the UIC 60 rails of the double track bridge were modeled with rectangular beam elements, giving cross sectional properties corresponding to the actual rail cross section. The element length was at most 0.5 m (both for bridge and rail elements) and each rail node was connected to the corresponding bridge node with a rigid link. The FE model of the bridge consisted of linear, elastic and isotropic materials. Support conditions were assumed according to bridge design documents, but also verified as reliable in previous work (Wiberg, 2009). Fig. 6 represents the boundary conditions, where the legend *F* indicates that the bridge deck and pier are fixed in translation movement. The main girder



Fig. 3. The spectacular New Årsta Bridge in Stockholm.

was released for longitudinal movements at other supports. The totally 24 Swiss mageba pot bearings had the function of hinges for free rotation about the transverse bridge deck axis. Torsional rotation of the bridge over piers was constrained to follow the bending of the oval piers in their stiff direction. Bridge deck rotation about the vertical axis over each pier was prevented due to the support consisting of two bearings in the transverse direction. The lower basis of all piers were assumed to be clamped but in reality the foundation blocks of P8 and P9 rested on concrete filled steel piles. A thorough description of the bridge with all sensor locations is found in Wiberg (2006).

## 4.2 The loadings

### 4.2.1 General

In this study the FE model was updated using tests with Swedish Rc6 locomotives. The updated model was then used to study the effect of passing high speed trains (HSLM) as specified in design codes.

### 4.2.2 The Rc6 locomotive

The updating process considered a field test with two Swedish Rc6 locomotives positioned at different locations in a static load test according to Wiberg (2009) and, in a dynamic load test, one locomotive crossing the bridge at different speeds. The locomotive is visualized in Fig. 7(a). Each of the four axles was represented as a point load of 19.5 tons and a



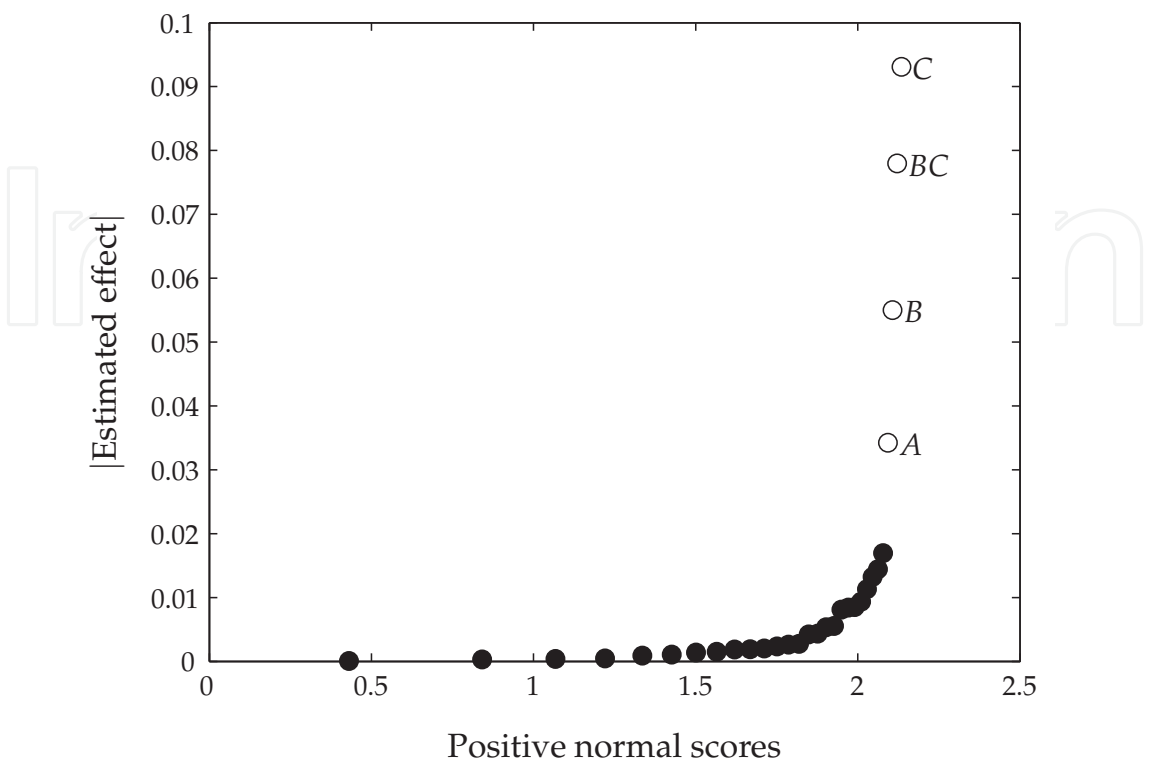


Fig. 4. Half normal plot with absolute values of estimated FE modeling parameter effect on vertical bridge deck acceleration. Factor definition: (A) damping ratio, (B) tendons and (C) vehicle speed.

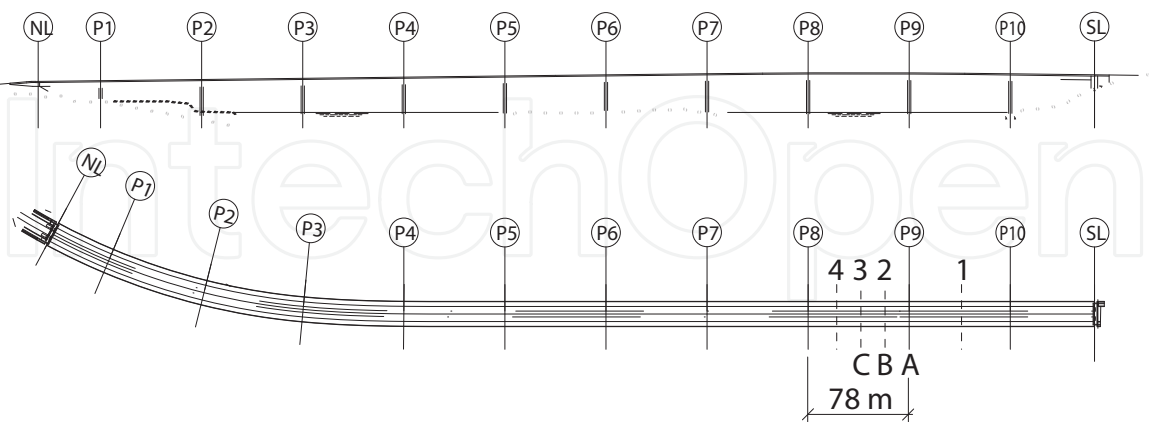


Fig. 5. Elevation and plan view of the New Årsta Bridge. Between the northern and southern abutment, NL and SL, respectively, the 10 piers are designated P1 to P10. Strain and acceleration sensor sections are marked A, B and C. Section 1, 2, 3 and 4 were used for vertical deflection measurements.

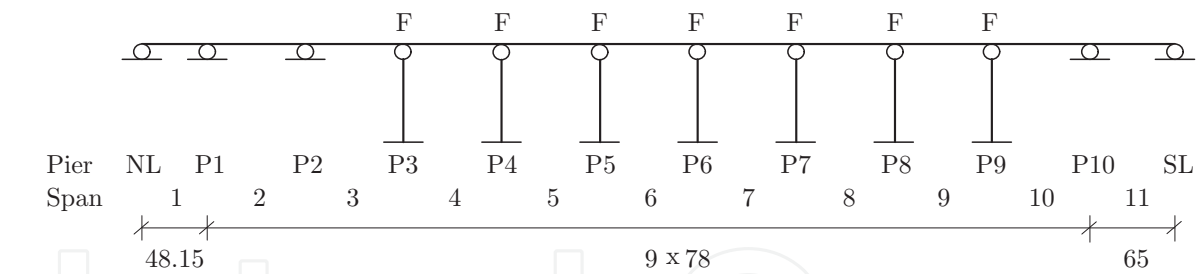
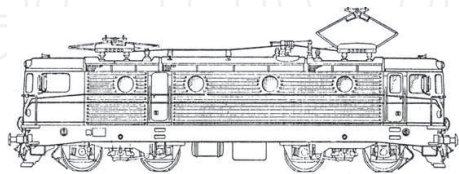
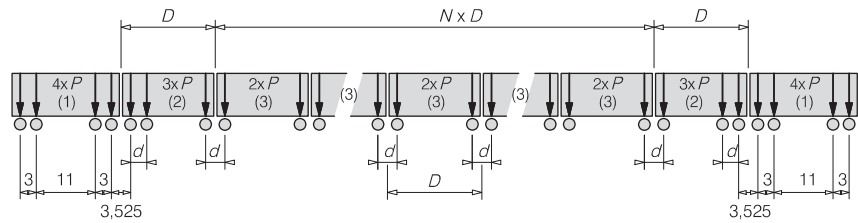


Fig. 6. Boundary conditions assigned to the bridge model.



(a) Rc6 locomotive.



(b) HSLM-A configurations.

Fig. 7. Representation of vehicle loads.

representative distribution in the moving load case using amplitude functions. The internal distance between the axles in a bogie was 2.7 m and the bogie center to center distance was 7.7 m.

### 4.2.3 The HSLM-A configurations

The high speed load models, intended for railway bridge simulations above 200 km/h, were adopted here to subject the optimized FE model for more extreme dynamics than the current maximum speed limit of 140 km/h across the bridge. Fig. 7(b) is used in Eurocode to represent the HSLM-A configurations (CEN, 2002). Appendix 5.1 specifies the varying number of intermediate coaches, coach lengths, bogie axle spacings and point forces between the 10 different HSLM-A configurations.

### 4.3 Model optimization

In dynamic modeling, the dynamic characteristics of the bridge are of main concern, i.e. natural frequencies, mode shapes and damping ratios, why those should be focused on in detail. For that purpose, the objective function of Zárate & Caicedo (2008) would be optimal:

$$\Pi = \sum_{i=1}^n \left[ \left[ 1 - \text{MAC} \left( \phi_{mi}, \phi_i \left( \mathbf{p}_j \right) \right) \right] + \left| \frac{f_{mi} - f_i \left( \mathbf{p}_j \right)}{f_{mi}} \right| \right] \quad (9)$$

However, as the modal assurance criterion (MAC) values were unavailable the objective function in Eq. 6 was considered instead. No focus was placed in evaluating different objective functions and the influence of variations in standard deviations (weight).

All 6 modeling parameters in Wiberg et al. (2009), i.e. damping ratios, modulus of elasticity, rails, tendons, vehicle speed and mass density, were significantly influencing typical dynamic load effects and the dynamic properties of the bridge. Therefore, they were all included in the optimization process. Damping and vehicle speed were obviously only considered in the dynamic analyzes. The importance of rails and tendons was analyzed based on their inclusion or exclusion in the FE model. The material properties of the rails and tendons were assumed as known. The prestress effect was included in a geometrically nonlinear large displacement analysis preceding each linear FE model restart execution for static and dynamic load effects. Modal damping was used in mode superposition of the moving load simulations. Thus, in the calculation of the mode shapes and frequencies, the effects of the axial compressive load on the modes and frequencies are included since the numerical calculation is based on the configuration at the start of the restart analysis. The linear mode superposition analysis that followed were then based on these mode shapes and frequencies, resulting in a dynamic response relative the prestressed bridge configuration.

In Table 1 the frequency columns from left to right are results from: an initial and manually tuned FE model in Wiberg (2006) but without rails and tendons, fast Fourier transforms of acceleration signals in Wiberg (2006), enhanced frequency domain decompositions from operational modal analysis in Wiberg & Karoumi (2009) and stochastic subspace identifications from operational modal analysis in Wiberg (2007). A dash only (see EFDD in Table 1) means undetected, while the dashes with parentheses (see SSI-PC in Table 1) stands for detected but unstable in the stabilization diagram as a result of operational modal analysis in Wiberg (2007). As can be seen from Table 1, already a simple manual updating resulted in a correct estimation of natural frequencies. However, the obtained high equivalent modulus of elasticity was questioned and therefore object of optimized updating. In addition, the initial manually tuned FE model used boundary conditions proven to be somewhat inaccurate according to Wiberg (2009). Henceforth, the notations differ between initial,  $FE_{\text{initial}}$ , initial manually tuned,  $FE_{\text{tuned}_1}$ , final manually tuned,  $FE_{\text{tuned}_2}$ , and optimized FE model,  $FE_{\text{optimized}}$ .

The optimization process was performed in the following two steps, based on the final manually tuned FE model:

1. Identification of updated material parameters (modulus of elasticity and mass density) from static load tests for strain and deflection residuals, together with frequency residuals.
2. Identification of modal damping ratio from dynamic load tests with maximum and root mean square (rms) acceleration residuals.

The frequency residuals were based on FE solutions using the subspace iteration method carried out for the structure linearized at the start of the restart analysis after prestress. The frequencies  $f_1$  and  $f_5$  at 1.3 Hz and 3.55 Hz were used, see Table 1. Strain residuals were based on axial beam stresses. The FE code can be modified to include the constrained warping effect on stresses. This was not considered here as it is based on torsional curvatures, manually given from separate analyzes. To include them as updating parameters was tested but made

No.	Type	Predicted		Measured		
		FE <sub>initial</sub>	FE <sub>tuned<sup>a</sup><sub>1</sub></sub>	FFT <sup>a</sup>	EFDD <sup>b</sup>	SSI-PC <sup>c</sup>
1	bending	1.03	1.30	1.30	1.29	(-)
2	coupled	1.13	1.44	1.45	1.45	(-)
3	coupled	1.91	2.45	2.43	2.43	2.43
4	coupled	2.53	3.26	3.26	-	3.24
5	coupled	2.78	3.55	3.55	3.50	3.55

<sup>a</sup> Wiberg (2006)  
<sup>b</sup> Wiberg & Karoumi (2009)  
<sup>c</sup> Wiberg (2007)

Table 1. Natural frequencies (Hz) from measured acceleration signals and for an initial and manually tuned FE model.

the optimizing algorithm unstable. However, the effect of unconstrained warping is relatively small in this case, see Wiberg (2009).

Frequency residuals only, strain residuals only, deflection residuals only, acceleration residuals only and their combinations were studied independently according to the principle:

$$\left\{ \begin{array}{l} \mathbf{p}_1 = \left( \frac{E_j}{E_0}, \frac{\rho_j}{\rho_0} \right) \\ \mathbf{z}_1 = (f_1, f_5, \varepsilon_1, \dots, \varepsilon_{51}, v_1, \dots, v_{20}) \end{array} \right\}$$

(10)

$$\left\{ \begin{array}{l} \mathbf{p}_2 = \left( \frac{\zeta_j}{\zeta_0} \right) \\ \mathbf{z}_2 = (a_1, \dots, a_3) \end{array} \right\}$$

(11)

with the indexes 1 and 2 on **p** and **z** corresponding to the two different optimization steps. Thus, Eq. 10 was used with 2 frequencies, 51 strains and 20 deflections all together included, but also for frequencies, strains and deflections separately. Unfortunately, none of the installed axial strain transducers was active during the dynamic load testing. Therefore, according to Eq. 11, modal damping was tuned against acceleration residuals only, based on the three monitoring sections of Fig. 5. The location of all sensors within the monitoring sections were considered redundant information here but is to be found in for example Wiberg (2006).

An educated guess of the initial vector of updating parameters was necessary. Based on the results of Wiberg (2006) and Wiberg (2009), manually tuned start values of  $E_0 = 55$  GPa and  $\rho_0 = 2500$  kg/m<sup>3</sup> were used for modulus of elasticity and mass density, respectively, and a constant damping ratio of  $\zeta_0 = 0.01$  was assigned to all modes and used in the mode superposition procedure. This corresponds to the modal damping ratio found for prestressed bridges in design codes (see CEN (2002)).

All load testing used Rc6 locomotives and is described in detail in Wiberg (2009). Mode superposition was used to calculate the responses of the simulated Rc6 locomotive crossings with a time step of  $\Delta t = 5$  ms. The initial implicit time integration in the geometrically

nonlinear axial load case operated on the basic equation of motion using the BFGS matrix update method algorithm (SOLVIA® Finite Element System, 2007).

Due to the restrictions of the beam FE model, i.e. using a beam element node to compare accelerations at the locations of accelerometers in the cross section, these signals were not comparable in the first place. Measured and modeled acceleration signals from the crossing Rc6 locomotive were therefore first low-pass filtered with a Butterworth filter at 5 Hz and then smoothed, using Savitzky-Golay filtering. Generally, a FE model is not optimal in reproducing high frequency content, especially not in representing a complex structure with a simple beam as is the case here. The low-pass filter at 5 Hz for reasonable acceleration comparison was therefore motivated. A Savitzky-Golay smoothing filter was chosen as they typically are used for a noisy signal whose frequency span (without noise) is large and they are considered optimal in the sense that they minimize the least-squares error in fitting a polynomial to frames of noisy data (The MathWorks, Inc., 2009).

To remove the rotational accelerations due to torsion, the measured signals from two accelerometers, 1 and 2, at the same distance from the center of gravity but on opposite sides were combined to compute the vertical translation acceleration only according to:

$$a_b = \frac{a_1 + a_2}{2} \quad (12)$$

In this way, assuming an infinitely stiff cross section, predicted vertical node accelerations were directly comparable with the measured bending acceleration  $a_b$  in monitoring section C, see Fig. 5. However, with only one accelerometer in monitoring section B, the predicted total vertical acceleration  $a_{tot}$  for comparison with measurements was calculated from beam node accelerations as:

$$a_{tot} = a_b + L \cdot a_r \quad (13)$$

with  $a_b$  the bending acceleration at center of gravity,  $a_r$  the rotational acceleration around the axial beam axis through center of gravity and  $L$  the distance perpendicular to the vertical axis, from center of gravity to the measuring position.

#### 4.4 Relevant moving load simulations

After optimization, resulting in updated modulus of elasticity, mass density and modal damping ration, the FE model was finally subjected to all ten HSLM-A configurations for more reliable moving load simulations. These load configurations crossed the bridge as point loads with corresponding amplitude functions on the outermost track solely, moving from NL to SL, at speeds between 100 and 250 km/h. Typical results of interest were bridge deck deflection, acceleration and bending moment. These were all estimated and evaluated in more detail for the most critical HSLM configurations.

### 5. Results and discussion

#### 5.1 Model optimization

The optimization algorithm operated efficiently but it was found unattainable to include all measurements in the response vector simultaneously. This was basically since the large-scale simplified model is incapable of predicting results based on all monitoring sections in Fig. 5



Parameter	FE <sub>init</sub>	FE <sub>tuned<sub>1</sub></sub>	FE <sub>tuned<sub>2</sub></sub>	FE <sub>optimized</sub>
Modulus of elasticity (GPa)	36	55	55	60
Mass density (kg/m <sup>3</sup> )	2500	2400	2500	2700
Modal damping ratio (%)	-	-	1.0	0.92;2.10
Rail	excluded	excluded	included	included
Tendons	excluded	excluded	included	included
Boundary condition	state 1	state 1	state 2	state 2

Table 2. Differences between updating parameters of initial, manually tuned and optimized FE model. Modal damping ratios for the optimized FE model corresponds to rms and maximum acceleration, respectively.

with its restrictions as a beam model and the relatively few number of updating parameters chosen for the FE model. In addition, some sensors and deflection measurements resulted in result distortion, probably due to a difference in assumed sensor position or other sources of errors. Frequencies and load effects are also non stationary due to time dependent effects, not considered in the FE model and therefore influencing the optimization accuracy since the measurements took place at different occasions.

The mean result of adding the updating parameter vector from the frequency optimization procedure separately, the deflection optimization procedure separately and the strain optimization procedure separately, constituted the updating parameter values of modulus of elasticity and mass density in the optimized FE model. Consequently, these three different objective function contributors, separately gave different optimized updating parameter values of modulus of elasticity and mass density. Notice therefore, if the intention for example is superior dynamic characteristics, it would have been better to concentrate on the frequency residuals solely, complemented with mode shape information. However, the intention here was again to implement the algorithm and investigate the possibilities with a simplified FE model.

The results of the optimized updating parameters are summarized in Table 2 as parameter value or structural condition before and after optimization. Obviously, the optimized values of modulus of elasticity and mass density had a negligible influence concerning the frequencies. This was reasonable as Table 1 already indicated good agreement in frequencies between measurements and manually tuned FE model. Therefore, the bending stiffness to mass ratio for the final manually tuned FE model at iteration start (55/2500) was similar to the ratio of the converged optimized FE model at (60/2700) in the typical iteration sequence of Fig. 8. Still, frequencies were included in the objective function to account for the change in structural system concerning the inclusion of rails and tendons.

The increased values in modulus of elasticity and mass density were believed to have a larger effect in the optimization based on static strains and deflections. Table 3 summarizes results for static strains and deflections as initially predicted, predicted with the optimized FE model and measured. Observe that strain results are exemplified with the values of one single strain transducer and its position in that monitoring section (A, B or C) according to Fig. 5 for one of the six different static load test configurations in Wiberg (2009). Deflections were presented

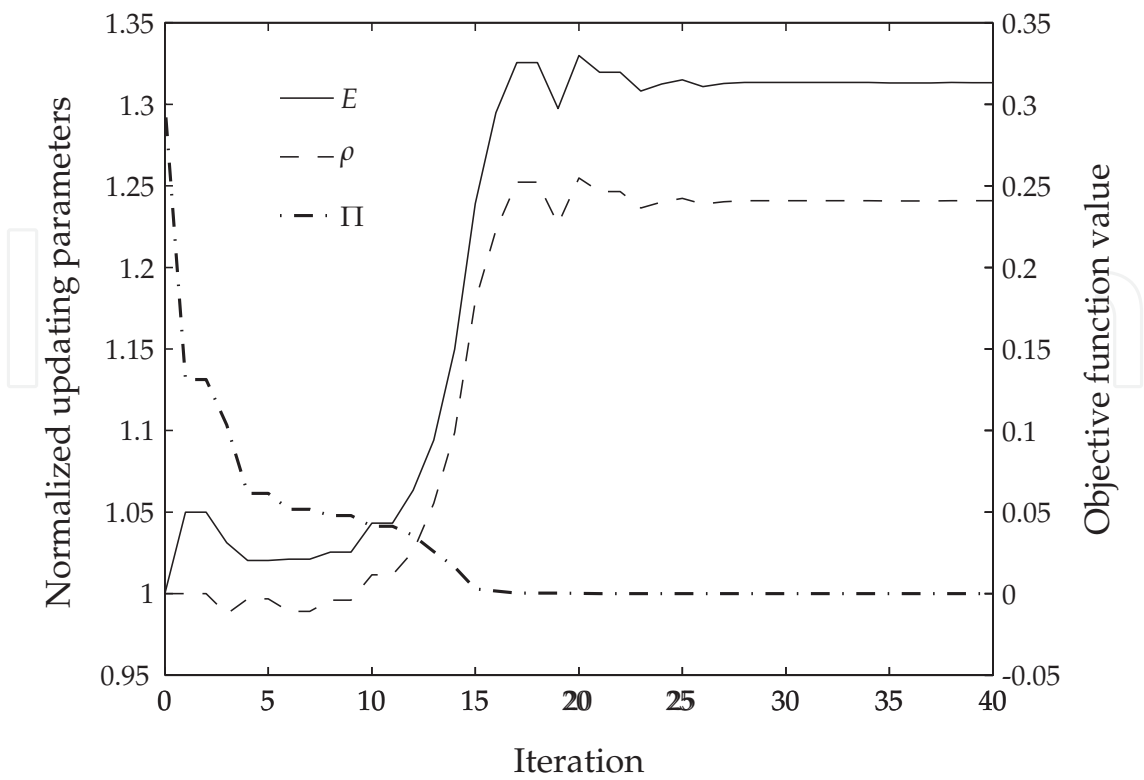


Fig. 8. Typical iteration sequence for optimization according to frequency residuals separately.

for the largest residual between initial FE model prediction and measured mean deflection in the point of interest (1, 2, 3 or 4) in Fig. 5. Notice that the initial FE model gave results on the safe side in all cases, while the updated FE model tended to be too optimistic, i.e. gave smaller load effect values than the measured ones.

Results for accelerations, based on the optimized values of modal damping ratios in Table 2, are presented in Table 4 for both measured, maximum and rms predicted acceleration. The corresponding acceleration signals are shown in Fig. 9. These signals represent a complete Rc6 locomotive crossing from SL to NL, traveling in outer curve at a speed of 120 km/h. Observe that the measured acceleration in the top of Fig. 9 is based on the signal manipulation according to Eq. 12. However, the way the measured signal looks may indicate that it still has some torsional acceleration included, i.e. that the beam element assumption of a rigid cross section with negligible in-plane stresses may not be completely satisfactory for the studied section. To be correct, a volume or shell element model of part of the bridge is necessary to include typical local flange modes, probably influencing the edge beam but are completely missed with the stiff cross section of the beam element. Consequently, it seems reasonable to base an optimized damping ratio on maximum acceleration for comparison with design codes, as those specify requirements on the maximum acceleration. However, in this case the predicted maximum acceleration may be too low due to the discretization and solution errors.

Even if the optimized model did not reproduce measured responses with highest accuracy in all cases it was considered reliable for the type of dynamic analysis assigned in design codes. At the same time, this is likely to be as far as one can get with a simplified FE model. It was not the intention with the simplified model in the first place to most accurately

Static load effect	FEA <sub>initial</sub>	FEA <sub>optimized</sub>	Measured
Strain A (10 <sup>-6</sup> )	37.9	22.7	23.2
Strain B (10 <sup>-6</sup> )	2.8	1.7	1.8
Strain C (10 <sup>-6</sup> )	16.9	10.2	11.1
Deflection 1 (mm)	4.3	2.6	3.0
Deflection 2 (mm)	5.8	3.5	4.0
Deflection 3 (mm)	9.5	5.7	6.5
Deflection 4 (mm)	5.8	3.5	3.5

Table 3. Modeled and measured static strains and deflections.

FEA <sub>initial</sub>	FEA <sub>initial</sub>	FEA <sub>optimized</sub>	FEA <sub>optimized</sub>	Measured	Measured
max	rms	max	rms	max	rms
0.01630	0.00387	0.01195	0.00303	0.01195	0.00303

Table 4. Modeled and measured vertical accelerations (m/s<sup>2</sup>) in the center of gravity of monitoring section C, filtered with a low pass filter at 5 Hz.

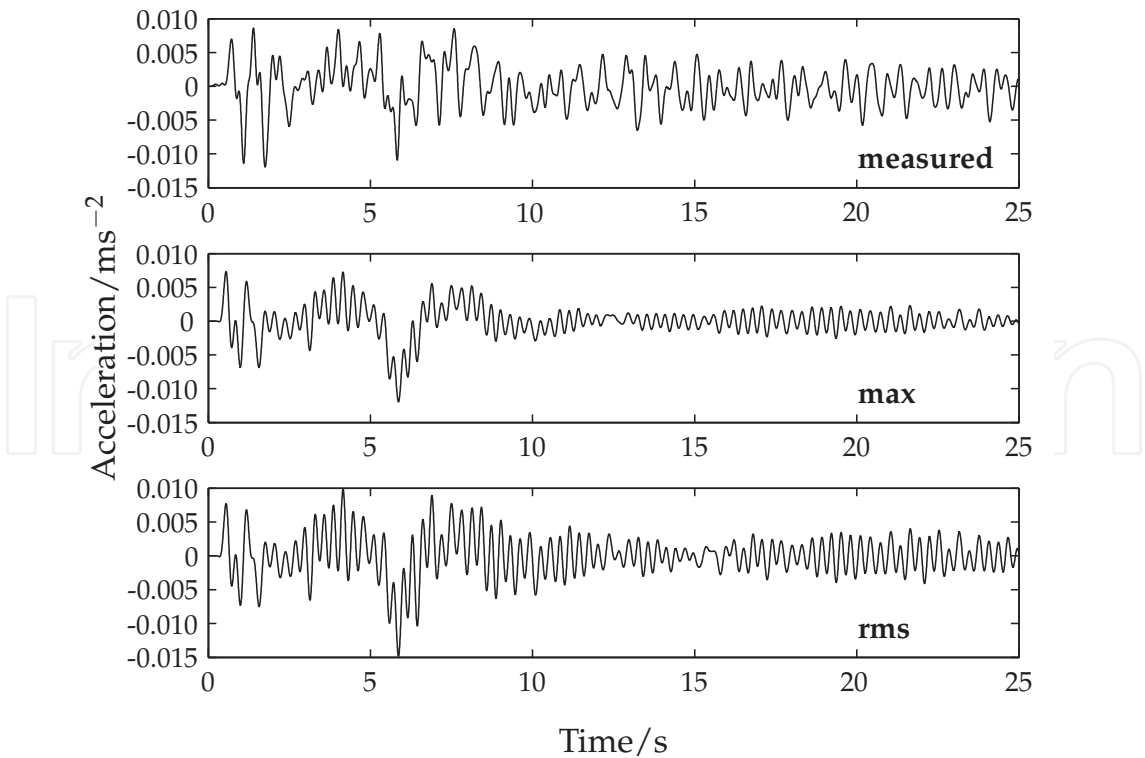


Fig. 9. Measured acceleration signal together with maximum and rms acceleration of the optimized FE model. All signals are filtered with a low pass filter at 5 Hz.

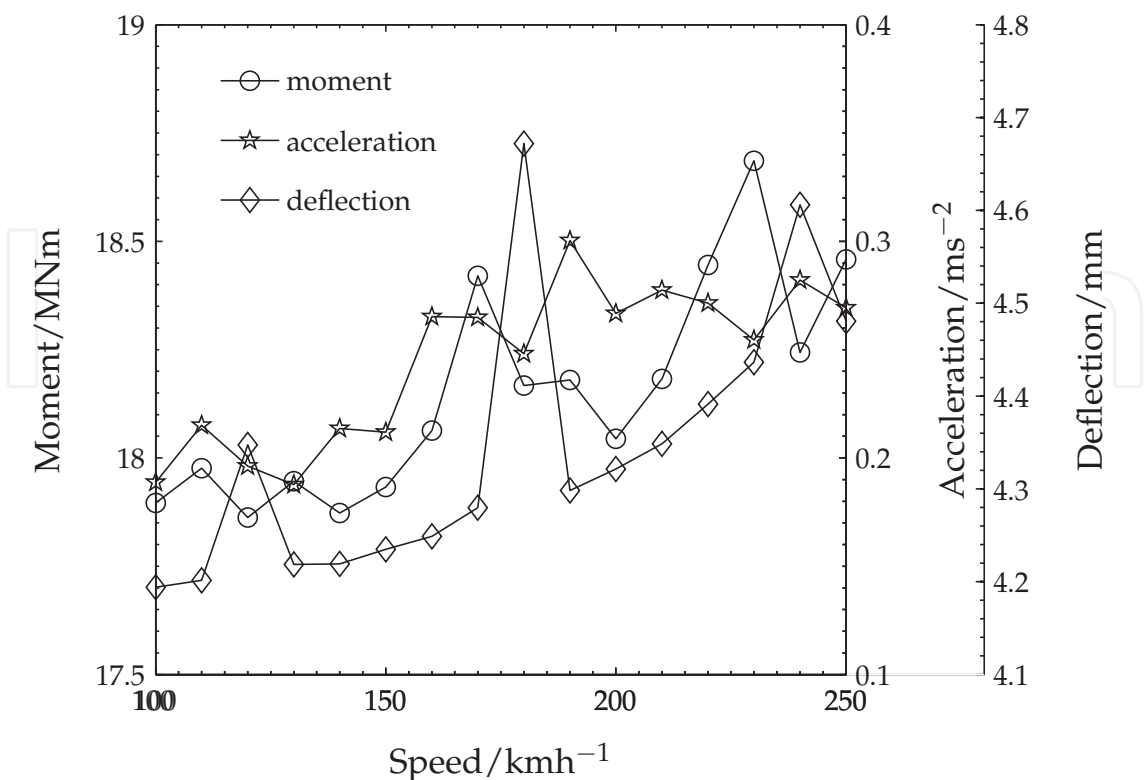


Fig. 10. Envelopes for bridge deck bending moment, vertical acceleration and deflection among all ten HSLM-A configurations with a speed increment of 10 km/h.

predict measurements. The main objective was to implement the optimization methodology and procedure in combination with statistical techniques to identify individually and jointly influencing FE modeling parameters to perform time efficient and relevant moving load simulations. In addition, the number and choice of updating parameters and the content of the objective function influence the possibilities of the adopted model.

Based on the optimized FE model, moving load simulations were performed with the ten HSLM-A train loads for increased accuracy in dynamic load effect predictions. Fig. 10 illustrates the envelope results for bridge deck bending moment, vertical acceleration and vertical deflection with a speed increment of 10 km/h between 100 km/h and 250 km/h. The most critical configurations were identified in Fig. 11 and found to be HSLM-A2, HSLM-A7 and HSLM-A10, respectively. For those three train loads, new results were presented in Fig. 12 for a speed increment of 5 km/h. Finally, the identified critical speeds in Fig. 12 were used to predict the load effects, at the critical location found in Fig. 13, from complete train crossings in time domain. The critical speeds corresponded to 165 km/h, 240 km/h and 180 km/h for HSLM-A2, HSLM-A7 and HSLM-A10, respectively.

Moments and accelerations showed relatively small differences compared to results using the initial FE model. However, deflections were considerably smaller compared to the results of the initial FE model according to Fig. 14. The optimized FE model corresponded to a dynamic amplification factor of 1.15 in deflection, compared to 1.09 for the initial FE model. Observe that these results are given for the node with maximum vertical acceleration. Obviously, the dynamic amplification can be larger elsewhere.

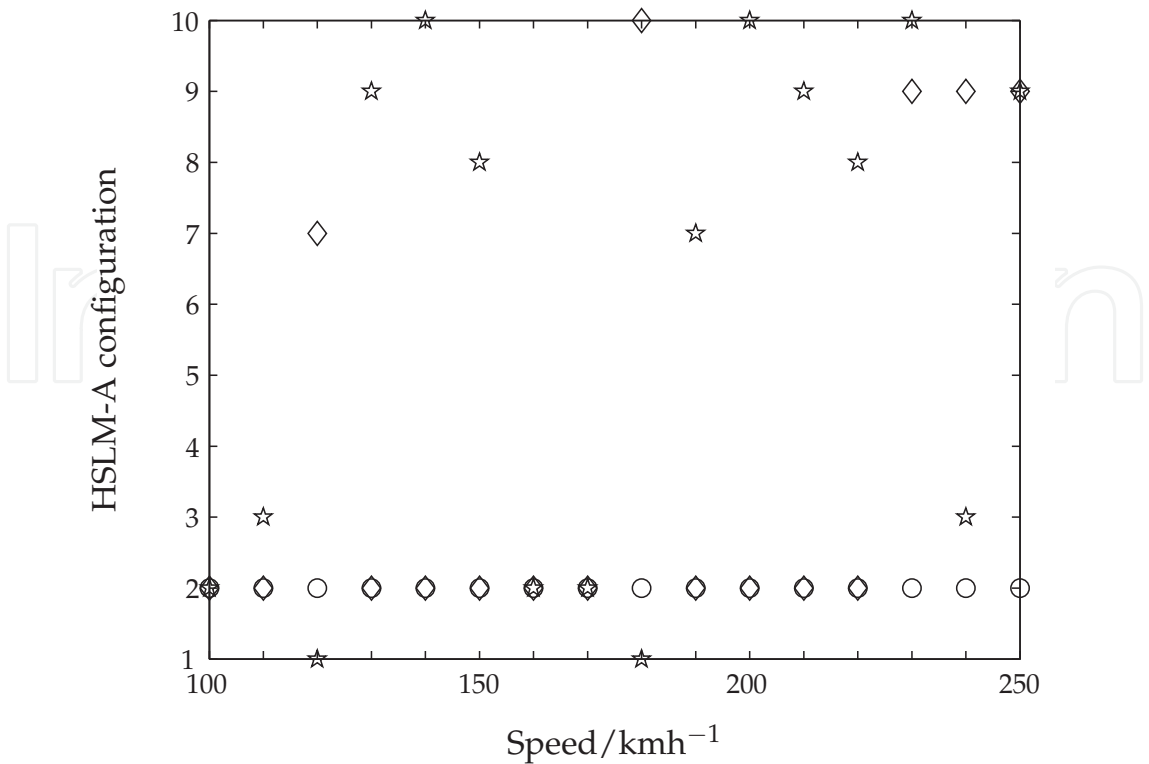


Fig. 11. Identification of the HSLM-A configurations corresponding to the envelope results. Bending moment is symbolized with (○), vertical acceleration with (☆) and vertical deflection with (◇).

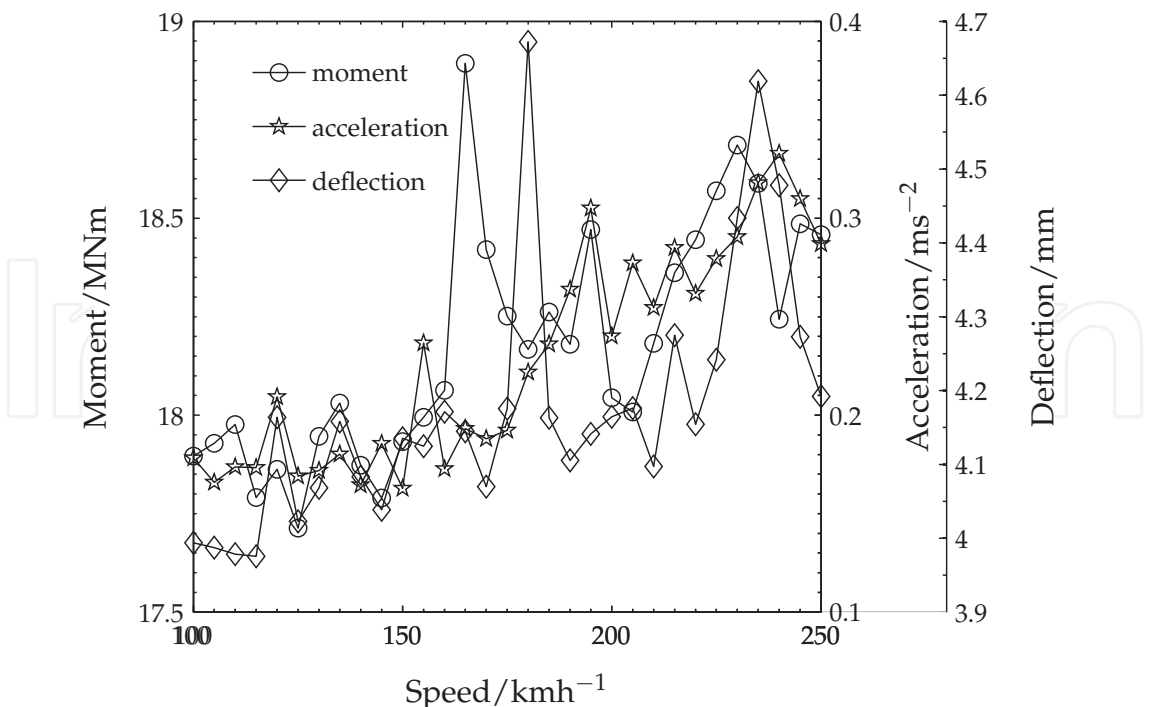


Fig. 12. The three most critical HSLM-A configurations, corresponding to HSLM-A2, HSLM-A7 and HSLM-A10, respectively, for bridge deck bending moment, vertical acceleration and deflection. A speed increment of 5 km/h was used.



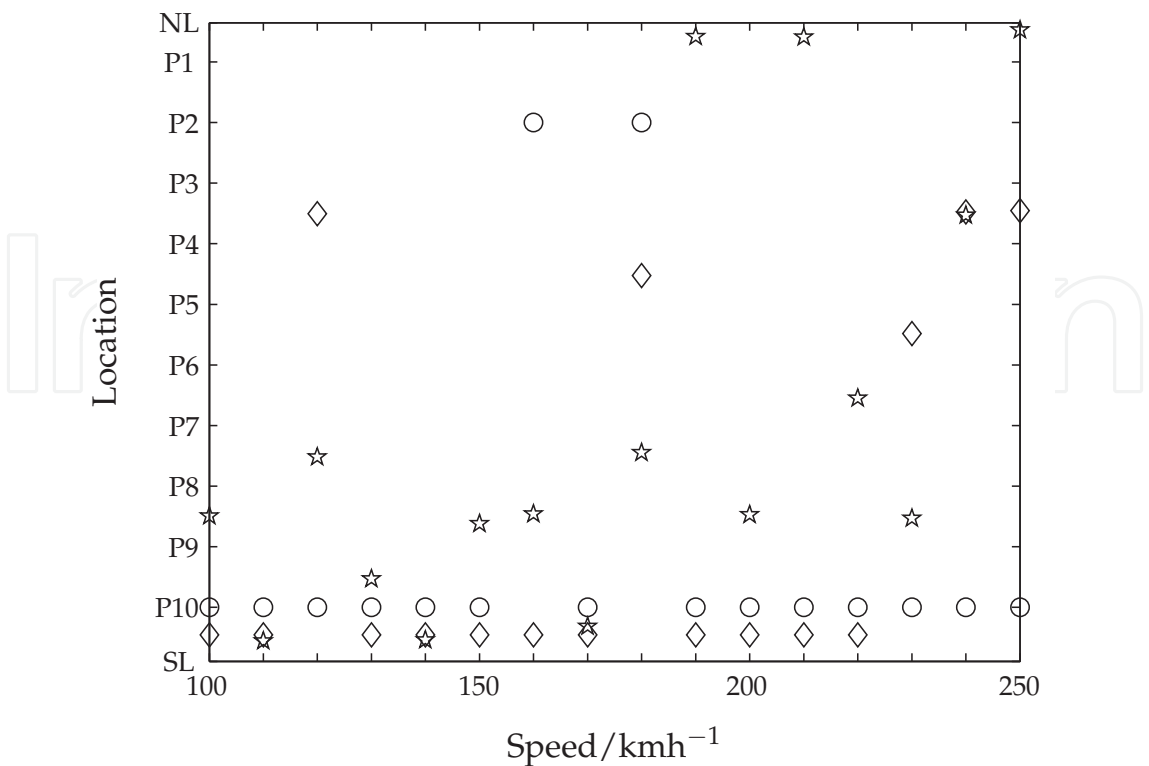


Fig. 13. Identification of bridge deck location of maximum bending moment, vertical acceleration and deflection of HSLM-A2, HSLM-A7 and HSLM-A10. Bending moment is symbolized with (○), vertical acceleration with (☆) and vertical deflection with (◇).

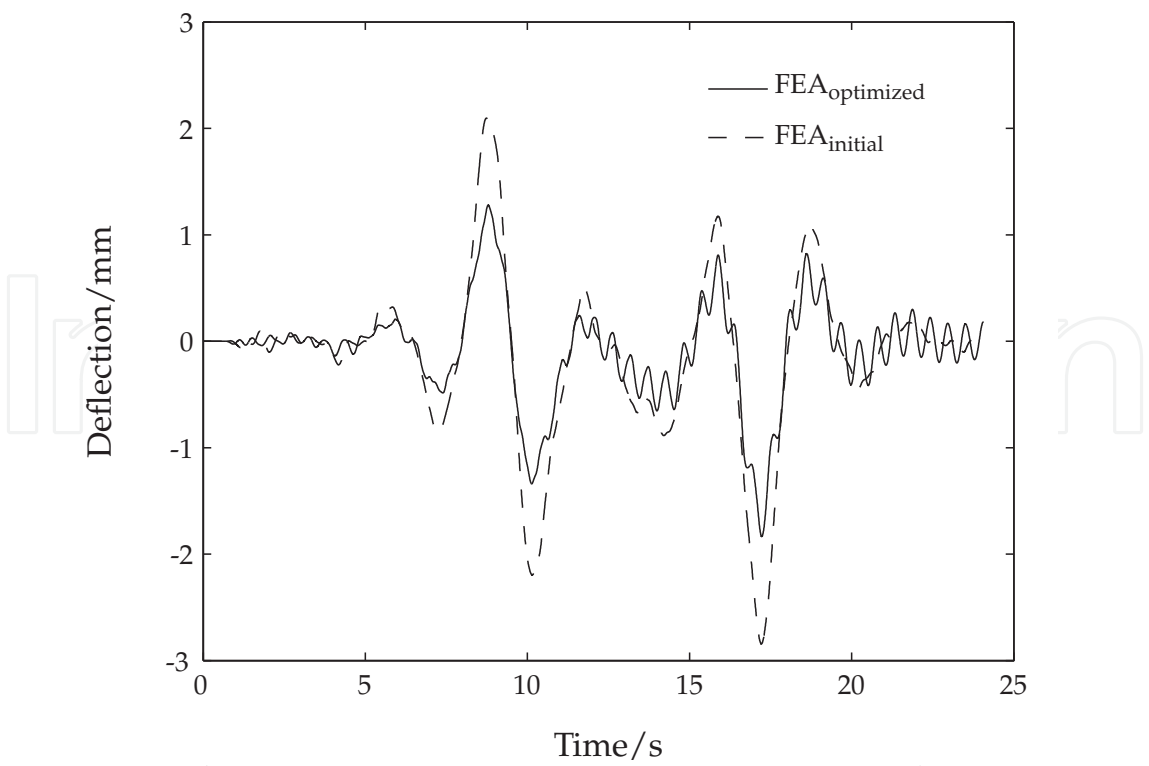


Fig. 14. Vertical deflection at the most critical node, i.e. midspan P4-P5 , for HSLM-A10 at 180 km/h.

## 6. Conclusions

Railway bridge design codes require detailed analyzes of passing trains at high speeds. Such analyzes are very time consuming as it involves many simulations using different train configurations passing at different speeds. Thus, simplified bridge and train models are chosen for time efficient simulations.

In this chapter a large-scale simplified railway bridge FE model for time efficient moving load simulations was optimized. The optimization uses natural frequencies from operational modal analysis and load effects from load testing, based on previously identified updating parameters. The optimization algorithm was easily implemented for FE model updating and was shown to operate efficiently in a benchmark test and for the specific bridge. The importance and the potential of optimization procedures in FE modeling for increased accuracy in moving load simulations is highlighted. Further, it was generally concluded that:

- Based on individually and jointly influencing factors, the optimized FE model predicted static and dynamic load effects more accurately.
- Even though the updated FE model predicted too optimistic load effects, i.e. not being on the safe side, the updated model resulted in larger dynamic amplification factor in comparison with the initial model.
- The optimized FE model predicted static load effects most accurately. The natural frequencies were already accurately calculated for the manually tuned FE model.
- The previously questioned high-valued equivalent modulus of elasticity was proven to be reasonable.
- Reliable modal damping ratios of 0.92% and 2.10%, for rms and maximum bridge deck acceleration, respectively, were predicted.
- Even if the simplified FE model in some sense is insufficient in load effect predictions, it stands for better predictions when optimization is used.
- More measured dynamic characteristics (natural frequencies, mode shapes and modal damping ratios), complementing updating parameters and a more detailed FE model are necessary for dynamic load effect predictions with highest accuracy.

To conclude, the author strongly recommend the working procedure of (1) manual FE model tuning, (2) updating parameter identification, and (3) final optimization focused on the result of interest and therefore based on a suitable objective function with that intention.

Finally, this chapter highlights the potential of the adopted optimization procedure. This methodology can not only be used for model updating based on measurements, but also be introduced and customized to work already in the bridge design phase for better (based on design code requirements) and more cost-effective designs.

7. Appendix

A. Benchmark input

The following input are used in the Benchmark test:

- Masses:
- $m_1 = 1000 \text{ kg}$   
 $m_2 = 20000 \text{ kg}$
- Initial velocity:
- $v = 30 \text{ m/s}$
- Initial displacement of  $m_2$ :
- $\delta = 0.05 \text{ m}$
- Stiffness:
- $k = 4 \cdot 10^6 \text{ N/m}$
- Damping:
- $c = 1 \cdot 10^5 \text{ Ns/m}$
- Time step:
- $\Delta t = 0.5 \text{ ms}$
- Beam section properties:
- $A = 0.06128 \text{ m}^2$   
 $I = 0.01573 \text{ m}^4$
- Material properties:
- $E = 210 \text{ GPa}$   
 $\nu = 0.3$   
 $\rho = 16000 \text{ kg/m}^3$

B. HSLM-A

Universal Train	Number of intermediate coaches  $N$	Coach length $D$ (m)	Bogie axle spacing $d$ (m)	Point force $P$ (kN)
A1	18	18	2.0	170
A2	17	19	3.5	200
A3	16	20	2.0	180
A4	15	21	3.0	190
A5	14	22	2.0	170
A6	13	23	2.0	180
A7	13	24	2.0	190
A8	12	25	2.5	190
A9	11	26	2.0	210
A10	11	27	2.0	210

### C. Notation

The following symbols are used in this chapter

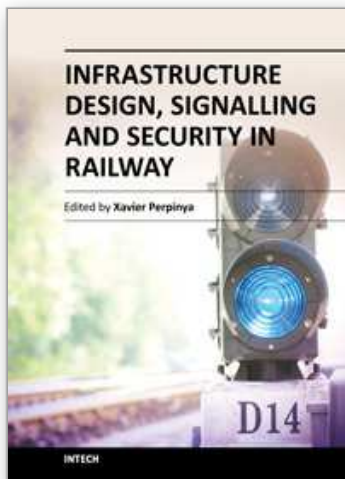
- $a$  = acceleration ( $\text{m/s}^2$ );
- $A$  = cross section area ( $\text{m}^2$ );
- $E$  = modulus of elasticity (Pa);
- $f$  = natural frequency (Hz);
- $n$  = mode number;
- $N$  = response vector length;
- $p$  = elements of  $\mathbf{p}$ ;
- $\mathbf{p}$  = updating parameter vector;
- $v$  = vertical deflection (m);
- $w$  = elements of  $\mathbf{W}$ ;
- $\mathbf{W}$  = weighting matrix;
- $\mathbf{z}$  = response vector;
- $\varepsilon$  = axial strain;
- $\zeta$  = equivalent modal critical damping ratio;
- $\Pi$  = scalar objective function value;
- $\rho$  = mass density ( $\text{kg/m}^3$ );
- $\sigma$  = standard deviation;
- $\phi$  = natural vibration mode;
- $\omega$  = circular frequency (rad/s);

### 8. References

- CEN (2002). *Eurocode 1: Actions on structures – Part 2: Traffic loads on bridges (prEN 1991-2)*.
- Coleman, T. F. & Zhang, Y. (2009). *Optimization Toolbox™ 4 User's Guide*, The MathWorks, Inc.
- Friswell, M. I. & Mottershead, J. E. (1995). *Finite Element Model Updating in Structural Dynamics*, Springer.
- Jaishi, B. & Ren, W. X. (2005). Structural finite element model updating using ambient vibration test results, *J. Struct. Engrg.* 131(4): 617–628.
- Jonsson, F. & Johnson, D. (2007). *Finite Element Model Updating of the New Svinesund Bridge. Manual Model Refinement with Non-Linear Optimization*, Msc thesis, Chalmers University of Technology, Sweden.
- Lagarias, J. C., Reeds, J. A., Wright, M. H. & Wright, P. E. (1998). Convergence properties of the nelder-mead simplex method in low dimensions, *SIAM Journal of Optimization* 9(1): 112–147.
- Mottershead, J. E. & Friswell, M. I. (1993). Model updating in structural dynamics: A survey, *Journal of Sound and Vibration* 167(2): 347–375.

- Schlune, H., Plos, M. & Gylltoft, K. (2009). Improved bridge evaluation through finite element model updating using static and dynamic measurements, *Engineering Structures* 31(7): 1477–1485.
- SOLVIA® Finite Element System (2007). Users Manual Version 03.
- The MathWorks, Inc. (2009). *Signal Processing Toolbox™ 6 User's Guide*.
- Wiberg, J. (2006). *Bridge Monitoring to Allow for Reliable Dynamic FE Modelling. A Case Study of the New Årsta Railway Bridge*, Lic thesis, Royal Institute of Technology, Sweden.
- Wiberg, J. (2007). Railway bridge dynamic characteristics from output only signal analysis, *Proc., Int. Conf. on Experimental Vibration Analysis for Civil Engineering Structures (EVACES'07)*, Porto, Portugal.
- Wiberg, J. (2009). An equivalent modulus of elasticity approach for simplified modelling and analysis of a complex prestressed railway bridge, *Advances in Structural Engineering*. Submitted.
- Wiberg, J. & Karoumi, R. (2009). Monitoring dynamic behaviour of a long-span railway bridge, *Structure and Infrastructure Engineering* 5(5): 419–433.
- Wiberg, J., Karoumi, R. & Pacoste, C. (2009). Statistical screening of individual and joint effect of several modeling factors on the dynamic fe response of a railway bridge, *Structural Control and Health Monitoring*. Submitted.
- Willis (1850). Deflexion of railway bridges under the passage of heavy bodies, *Journal of the Franklin Institute* 49(1): 7–8.
- Zárate, B. A. & Caicedo, J. M. (2008). Finite element model updating: Multiple alternatives, *Engineering Structures* 30(12): 3724–3730.





## **Infrastructure Design, Signalling and Security in Railway**

Edited by Dr. Xavier Perpinya

ISBN 978-953-51-0448-3

Hard cover, 522 pages

**Publisher** InTech

**Published online** 04, April, 2012

**Published in print edition** April, 2012

Railway transportation has become one of the main technological advances of our society. Since the first railway used to carry coal from a mine in Shropshire (England, 1600), a lot of efforts have been made to improve this transportation concept. One of its milestones was the invention and development of the steam locomotive, but commercial rail travels became practical two hundred years later. From these first attempts, railway infrastructures, signalling and security have evolved and become more complex than those performed in its earlier stages. This book will provide readers a comprehensive technical guide, covering these topics and presenting a brief overview of selected railway systems in the world. The objective of the book is to serve as a valuable reference for students, educators, scientists, faculty members, researchers, and engineers.

### **How to reference**

In order to correctly reference this scholarly work, feel free to copy and paste the following:

Johan Wiberg, Raid Karoumi and Costin Pacoste (2012). Optimized Model Updating of a Railway Bridge for Increased Accuracy in Moving Load Simulations, Infrastructure Design, Signalling and Security in Railway, Dr. Xavier Perpinya (Ed.), ISBN: 978-953-51-0448-3, InTech, Available from:

<http://www.intechopen.com/books/infrastructure-design-signalling-and-security-in-railway/optimized-model-updating-of-a-railway-bridge-for-increased-accuracy-in-moving-load-simulations>

**INTECH**  
open science | open minds

### **InTech Europe**

University Campus STeP Ri  
Slavka Krautzeka 83/A  
51000 Rijeka, Croatia  
Phone: +385 (51) 770 447  
Fax: +385 (51) 686 166  
[www.intechopen.com](http://www.intechopen.com)

### **InTech China**

Unit 405, Office Block, Hotel Equatorial Shanghai  
No.65, Yan An Road (West), Shanghai, 200040, China  
中国上海市延安西路65号上海国际贵都大饭店办公楼405单元  
Phone: +86-21-62489820  
Fax: +86-21-62489821

© 2012 The Author(s). Licensee IntechOpen. This is an open access article distributed under the terms of the [Creative Commons Attribution 3.0 License](https://creativecommons.org/licenses/by/3.0/), which permits unrestricted use, distribution, and reproduction in any medium, provided the original work is properly cited.

IntechOpen

IntechOpen